Inorg. Chem. **2005**, *44*, 232–241

Novel Chiral "Calixsalen" Macrocycle and Chiral Robson-type Macrocyclic Complexes

Jian Gao,*,† Joseph H. Reibenspies,‡ Ralph A. Zingaro,‡ F. Ross Woolley,† Arthur E. Martell,‡,§ and Abraham Clearfield‡

Department of Radiology, University of Texas Health Science Center, San Antonio, Texas 78229-3900, and Department of Chemistry, Texas A & M University, College Station, Texas 77843-3255

Received June 23, 2004

A family of novel chiral "calixsalen" Schiff base macrocycles *R,R*-H_3**L4**, *R,R*-H_3**L5**, containing three chiral diamino moieties were synthesized by an efficient self-assembly and characterized by ^{1}H and ^{13}C NMR, mass spectrometry, and X-ray diffraction. The systematic synthesis, structure, and coordination properties of the [2 + 2] and [3 + 3] Robson-type Schiff base macrocyclic mono-, di-, tri-, and tetranuclear metal complexes were explored.

Introduction

The presence of multinuclear sites has long been cited in an attempt to explain the function of many biologically important enzymes.[1] Substantial effort has been devoted to synthesizing model complexes that would permit the reliable simulation of enzyme behaviors experimentally to better understand their function. Schiff base Robson-type macrocycles containing two bridging phenol groups have been widely used to synthesize homo- and hetero-dinuclear complexes.[2] Most investigations of these metal complexes are an outgrowth of bioinorganic chemistry and enzymatic catalysis research.[3] Typically, Robson-type macrocyclic complexes have been derived from the template condensation of achiral diamines such as ethylenediamine or diethylenetriamine and 2-hydroxy-5-methyl-benzene-1,3-dicarbaldehyde. However, the use of chiral diamines such as 1*R*,2*R*-diaminocyclohexane (*R,R*-DACH), 1*R*,2*R*-diphenylethylenediamine (*R,R*-DPEN), and *R*-1,1′-binaphthalenyl-2,2′-diamine (*R*-BNDA) (see Scheme 1) in the construction of chiral Schiff base Robson-type macrocycles has received only limited study. Our primary interest in these compounds arises from the combination of the synthetic and structural chemistry of chiral macrocycles and how they differ from their achiral counterparts.[4] Unlike linear ethylenediamine for example, chiral diamine compounds have specific stereogenic conformation and structural rigidity (see Scheme 1). The conformational stability and shape persistency of chiral cyclic structures have been postulated to arise from the structural rigidity and chirality of their assembly moieties.[5] We speculated that a new type of chiral "calixsalen" macrocycle could be constructed using the characteristic of simultaneous self-assembly of the chiral diamines with 2-hydroxy-5-

Scheme 1

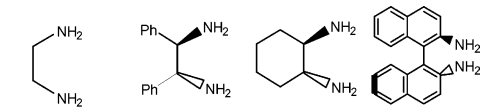

* To whom correspondence should be addressed. E-mail: gaoj2@uthscsa.edu.

† University of Texas Health Science Center.

‡ Texas A & M University.

§ Dr. Martell died suddenly in October of 2003. He laid the foundation that made this paper possible and contributed actively until his untimely passing.

(1) (a) Lippard, S. J.; Berg, J. M. In *Principles of Bioinorganic Chemistry*; University Science Books: Mill Valley, CA, 1994. (b) Cole, A. P.; Root, D. E.; Mukherjee, P.; Solomon, E. I.; Stack, T. D. P. *Science* **1996**, *273*, 1848. (c) Solomon, E. I.; Sundaram, U. M.; Machonkin, T. E. *Chem. Rev.* **1996**, *96*, 2563. (d) Feig, A. L.; Lippard, S. J. *Chem. Rev.* **1994**, *94*, 759.

(2) (a) Pilkington, N. H.; Robson, R. *Aust. J. Chem.* **1970**, *23*, 2225. (b) Das, R.; Nag, K. *Inorg. Chem.* **1991**, *30*, 2831. (c) Bosnich, B. *Inorg. Chem.* **1999**, *38*, 2554.

(3) (a) Long, R. C.; Hendrickson, D. N. *J. Am Chem. Soc.* **1983**, *105*, 1513. (b) Atkins, A.; Black, D.; Blake, A. J.; Marin-Becerra, A.; Persons, S.; Ruiz-Ramirez, L.; Schroder, M. *Chem. Commun.* **1996**, 457. (c) Yoncmura, M.; Usuki, N.; Nakamara, Y.; Ohba, M.; Okawa, H. *J. Chem. Soc., Dalton Trans.* **2000**, 3624.

(4) (a) Li, Z.; Jablonski, C. *Chem. Commun.* **1999**, 1531. (b) Chadim, M.; Budesinsky, M.; Hodacova, J.; Zavada, J.; Junk, P. C. *Tetrahedron: Asymmetry* **2001**, *12*, 127. (c) Kuhnert, N.; Strabnig, C.; Lopez-Periago, A. M. *Tetrahedron: Asymmetry* **2002**, *13*, 123.

(5) (a) Gawronski, J.; Kolbon, H.; Kwit, M.; Katrusiak, A. *J. Org. Chem.* **2000**, *65*, 5768. (b) Ricci, R.; Pasini, D. *Org. Biomol. Chem.* **2003**, *1*, 3261.

10.1021/ic049181m CCC: $30.25
Published on Web 12/24/2004

methyl-benzene-1,3-dicarbaldehyde. Successful construction of the larger chiral macrocycles by this approach is unique in supramolecular assembly[6] and chiral molecular recognition.[7]

Historically, achiral macrocyclic multinuclear complex models have been intensively investigated in bioinorganic catalysis, but their chiral counterparts have attracted relatively little attention. This paucity of research is striking given the predominance of metalloenzyme multinuclear centers located on the chiral backbone of polypeptides and proteins.[8] It may be that the larger body of existing achiral related data led researchers to build on more readily available information and thus place a disproportionate emphasis on achiral metal complexes. Another consideration is that the description of chiral multinuclear complexes in enzyme-like asymmetric catalysis is a relatively recent event. Although researchers are generally predisposed to expand upon such recent innovations, it is probable that there simply has not been sufficient time to produce chiral metal complexes in numbers close to their existing achiral counterparts.[9] Consequently, there are still comparatively few chiral multinuclear chelating ligands and structure-defined chiral multinuclear complexes currently available to inorganic biochemical researchers.

Members of our research group have studied the macrocyclic metal complexes for decades, focusing on their catalytic behavior in both bioinorganic and bioorganic chemistry.[10] Recently, we initiated a project specifically to study chiral macrocycle chemistry. Particular emphasis was placed on mimicking the distinctive function of enantioselective catalysis of natural enzymes.[11] Research aimed at increasing the body of knowledge about the synthesis and stereo structure of chiral metal complexes is critical to significantly increasing their utility. This paper reports on the synthesis and characterization of new chiral calixsalen macrocycles. The combination of calixarene and salen results in a stable chiral macrocycle with many multinuclear complexes. The template affects the coordination properties of a number of metal ions in the construction of the [2 + 2] and [3 + 3] macrocyclic complexes. They are discussed below on the basis of their crystallographic and spectroscopic characteristics.

Experimental Section

Materials and Measurements. All chemical reagents and solvents of analytical grade were obtained from Sigma-Aldrich Fine Chemicals Inc. Methanol and acetonitrile were desiccated by filtration through molecular sieves (4 Å) prior to use. ^{1}H NMR spectra were measured using a Unix-VMR-500 MHz spectrometer. Analyses for C, H, and N were processed on a Perkin-Elmer analyzer, model 240. Positive ion ESI-MS spectra were recorded employing LCQ electrospray mass spectrometry. The spectra were recorded over the mass range m/z 200−1000.

Synthesis of [(*R*,*R*-H_2L1)Ni(II)]$(ClO_4)_2$ (1). A solution of 2-hydroxy-5-methyl-1,3-benzenedicarboxaldehyde (0.1 mmol) was added dropwise to a solution containing $Ni(ClO_4)_2$ (0.05 mmol) and *R*,*R*-DPEN (0.1 mmol) in 10 mL of EtOH. After 4 h of stirring, a yellow product was obtained. Yield 66%. Anal. Calcd for $C_{50}H_{44}Cl_2N_6O_{10}Ni$: C 40.1, H 4.9, N 8.3. Found: C 40.2, H 5.0, N 8.2. Yellow crystals were obtained by the diffusion of MeOH into a MeCN solution of the sample.

Synthesis of [(*R*,*R*-L1)Ni_2(II)]$(ClO_4)_2\cdot 2CH_3CN$ (2). The complex was prepared by following a procedure similar to that described above using 2 equiv of Ni(II) as a template in the presence of 0.1 mmol of Et_3N. Yield 69%. Anal. Calcd for $C_{66.67}H_{60}Cl_{2.67}N_8O_{13.33}Ni_{2.67}$: C 55.7, H 4.2, N 7.8. Found: C 55.2, H 4.3, N 7.9.

Synthesis of [(*R*,*R*-H_2L1)Zn(II)]$(ClO_4)_2\cdot 2CH_3OH$ (3). A solution of 2-hydroxy-5-methyl-1,3-benzenedicarboxaldehyde (0.1 mmol) was added dropwise to a solution containing $Zn(ClO_4)_2$ (0.05 mmol) and *R*,*R*-DPEN (0.05 mmol) in 10 mL of EtOH. After 4 h of stirring, a yellow product was obtained. Yield: 66%. Anal. Calcd for $C_{48}H_{44}Cl_2N_4O_{12}Zn$: C 57.4, H 4.4, N 5.6. Found: C 57.3, H 4.6, N 5.7. Yellow crystals were obtained by diffusion of MeOH into a MeCN solution of the sample.

Synthesis of [(*R*,*R*-H_2L1)Zn_2(II)]$(ClO_4)_2\cdot 2CH_3OH$ (4). The complex was prepared by following a procedure similar to that described above, using 2 equiv of Zn(II) as a template in the presence of Et_3N. Yield: 78%. Anal. Calcd for $C_{46}H_{38}Cl_2N_4O_{10}Zn_2$: C 54.8, H 3.8, N 5.6. Found: C 55.0, H 4.2, N 5.7.

Synthesis of [(*R*,*R*-L1)Cu_2(II)]$(ClO_4)_2\cdot 2CH_3CN$ (5). The complex was prepared by following a procedure similar to that described above, using an equivalent of Cu(II) as a template. Yield:, 87%. Anal. Calcd for $C_{50}H_{44}Cl_2N_6O_{10}Cu_2$: C 55.2, H 4.1, N 7.7. Found: C 55.2, H 4.3, N 7.9.

Synthesis of [((*R*,*R*-L2)Co_2(III))$_2(OH)_2(OAc)_2$]$(ClO_4)_4\cdot 4CH_3OH$ (6). A solution of 2-hydroxy-5-methyl-1,3-benzenedicarboxaldehyde (0.1 mmol) was added dropwise to a solution containing 2 equiv of $Co(ClO_4)_2$ and 1*R*,2*R*-DACH (0.1 mmol) in 5 mL of MeCN. Stirring for 10 h resulted in a brown solution. To this system, 2 equiv of acetic acid was added in room air, and red crystals formed. Yield: 68%. Anal. Calcd for $C_{68}H_{91}Cl_4Co_4N_8O_{30}$: C 43.5, H 4.9, N 6.0. Found: C 43.4, H 4.7, N 6.1.

Synthesis of [Pb(II)L2](SCN)$_2\cdot 2CH_3OH$ (7). A solution of 2-hydroxy-5-methyl-1,3-benzenedicarboxaldehyde (0.10 mmol) was added dropwise to a solution containing $Pb(SCN)_2$ (0.05 mmol) and *R*,*R*-DACH (0.10 mmol) in 10 mL of MeOH. After refluxing for 4 h with magnetic stirring, the mixture was allowed to sit overnight, and yellow crystals were obtained. Yield: 55%. Anal. Calcd for $C_{34}H_{44}N_6O_4PbS_2$: C 46.8, H 5.1, N 9.6. Found: C 46.7, H 5.3, N 9.8.

(6) (a) Bushey, M. L.; Hwang, A.; Stephens, P. W.; Nuckolls, C. *Angew. Chem., Int. Ed.* **2002,** *41*, 2828. (b) Gallant, A. J.; Maclachlan, M. J. *Angew. Chem., Int. Ed.* **2003**, *42*, 5307. (c) Sidorov, V.; Kotch, F. W.; Ei-Kouedi, M.; Davis, J. T. *Chem. Commun.* **2000**, 2369. (d) Kim, Y.; Mayer, M. F.; Zimmerman, S. C. *Angew. Chem., Int. Ed.* **2003**, *42*, 1121.

(7) (a) Ito, K.; Noike, M.; Kida, A.; Ohba, Y. *J. Org. Chem.* **2002**, *67*, 7519. (b) Lin, J.; Zhang, H. C.; Pu, L. *Org. Lett.* **2002**, *4*, 3297. (c) Kim, S. G.; Kim, K. H.; Kim, Y. K.; Shin, S. K.; Ahn, K. H. *J. Am. Chem. Soc.* **2003**, *125*, 13819. (d) Wehner, M.; Schrader, T.; Finocchiaro, P.; Failla, S.; Consiglio, G. *Org. Lett.* **2000**, *2*, 605.

(8) (a) Sazinsky, M. H.; Bard, J.; Donato, A. D.; Lippard, S. J. *J. Biol. Chem.* **2004**, *279*, 30600. (b) Steitz, T. A.; Steitz, J. A. *Proc. Natl. Acad. Sci. U.S.A.* **1993**, *90*, 6498. (c) Hall, D. R.; Leonard, G. A.; Reed, C. D.; Watt, C. I.; Berry, A.; Hunter, W. N. *J. Mol. Biol.* **1999**, *287*, 383.

(9) (a) Trost, B. M.; Terrell, L. R. *J. Am. Chem. Soc.* **2003**, *125*, 338. (b) Shibasaki, M.; Yoshikawa, N. *Chem. Rev.* **2002**, *102*, 2187−2209. (c) Ready, J. M.; Jacobsen, E. J. *Angew. Chem., Int. Ed.* **2002**, *41*, 1374.

(10) (a) Menif, R.; Martell, A. E.; Squattrito, P. J.; Clearfield, A. *Inorg. Chem.* **1990**, *29*, 4723. (b) Jurek, P. E.; Martell, A. E. *Inorg. Chem.* **2000**, *39*, 1016. (c) Gao, J.; Reibenspies, J.; Martell, A. E. *Inorg. Chim. Acta* **2002**, *338*, 157. (d) Gao, J.; Reibenspies, J.; Martell, A. E. *Inorg. Chim. Acta* **2003**, *346*, 67.

(11) (a) Gao, J.; Martell, A. E. *Org. Biomol. Chem.* **2003**, *1*, 2795. (b) Gao, J.; Martell, A. E. *Org. Biomol. Chem.* **2003**, *1*, 2801. (c) Gao, J.; Rebenspies, J.; Martell, A. E. *Angew. Chem., Int. Ed.* **2003**, *42*, 6008. (d) Gao, J.; Zingaro, R. A.; Reibenspies, J. H.; Martell, A. E. *Org. Lett.* **2004**, *6*, 2453.

Synthesis of *R,R*-H_3L4 (8). To a stirred solution of 2-hydroxy-5-methyl-1,3-benzenedicarboxaldehyde (15 mmol) in MeCN (300 mL) was added 1*R*,2*R*-diphenylethylenediamine (DPEN) (15 mmol) in MeOH (200 mL) at −5 °C under argon. A yellow solid formed that was filtered off, washed with methanol, and placed in a sealed container with P_2O_2 placed on the bottom to serve as a desiccant and allowed to dry in air. Yield: 99%. Mp 244 °C. $[\alpha]^{25}_D = -16.1$ (*c* 0.01, CH_2Cl_2). ESI-MS *m*/*z*: 1021.3333 $(M + H)^+$. Calcd for $C_{69}H_{60}N_6O_3 + H^+$: 1021.4807. ^{1}H NMR ($CDCl_3$), δ 2.36 (s, 3H, CH_3-), 4.82 (s, 2H, NCH−Ph), 7.08−7.54 (m, 12H, Ph), 8.12 (s, 2H, HC═N). ^{13}C NMR (in $CDCl_3$), δ 20.90 (CH_3-), 67.32 (−CH-benzene), 124.50, 125.70, 127.92, 128.44, 130.57, 133.46 and 140.22 (benzene), 155.3 (benzene-OH), 163.7 (CH═N). Anal. Calcd $C_{69}H_{60}N_6O_3$: C, 81.2; H, 5.9; N, 8.2. Found: C, 81.3; H, 6.0; N, 8.1%.

Synthesis of *R,R*-H_3L5 (9). A solution of 1*R*,2*R*-diaminocyclohexane (DACH) (1.71 g, 15 mmol) in 200 mL MeOH was added dropwise to a solution of 2-hydroxy-5-methyl-1,3-benzenedicarboxaldehyde (15 mmol) in MeCN (300 mL) at −5 °C under argon. After the mixture stirred for 8 h, yellow precipitates formed. The yellow solid was subsequently filtered off, washed with methanol, and dried in air using the same method described above. Yield: 99%. Mp > 300 °C. $[\alpha]^{25}_D = -238.8$ (*c* 0.01, CH_2Cl_2). ESI-MS *m*/*z*: 727.4255 $(M + H)^+$. Calcd for $C_{45}H_{54}N_6O_3 + H^+$: 727.4337. ^{1}H NMR ($CDCl_3$), δ 1.46−2.01 (s, 4H, $-CH_2$-cyclohexane), 2.16 (s, 3H, $-CH_3-$Ph), 3.38 (s, 1H, NCH-cyclohexane), 3.53(s, 1H, NCH-cyclohexane), 6.95 (s, 2H, benzene), 7.27 (s, 1H, benzene), 7.68 (s, 1H, phenol), 8.24 (s, 1H, HC═N), 8.69 (s, 1H, HC═N). ^{13}C NMR (in $CDCl_3$), δ 20.56 (CH_3-benzene), 24.55, 33.68 and 33.37 ($-CH_2-$ of cyclohexane), 73.80, 75.53 (NCH− cyclohexane), 118.9 (benzene), 123.2 (benzene), 127.1 (benzene), 130.1 (benzene-CH_3), 135.0 (benzene), 156.4 (−CH-benzene), 163.8 (−CH-benzene). Anal. Calcd for $C_{45}H_{54}N_6O_3$: C, 74.4; H, 7.5; N, 11.6. Found: C, 74.3; H, 7.6; N, 11.6%.

Synthesis of *R*-H_2L6 (10). A solution of *R*-1,1′-binaphthalenyl-2,2′-diamine (R-BNDA) (284 mg, 1.0 mmol) in 50 mL of MeOH was added dropwise to a solution of 2-hydroxy-benzaldehyde (2.0 mmol) in MeCN (50 mL) at 25 °C under argon. After stirring the mixture for 8 h at 60 °C, yellow precipitates formed. The yellow solid was subsequently filtered off, washed with methanol, and dried in air again using the method described above. Yield: 90%. Mp > 300 °C. ESI-MS *m*/*z*: 493.19 $(M + H)^+$. Calcd for $C_{34}H_{24}N_2O_2 + H^+$: 493.57. Anal. Calcd for $C_{34}H_{24}N_2O_2$: C, 82.9; H, 4.9; N, 5.7. Found: C, 83.1; H, 4.9; N, 5.7%.

Synthesis of [Ni_3(II)L3]·$(ClO_4)_3$ (11). Starting with a 5 mL methanol solution of *R,R*-H_3**L3** (0.1 mmol), 0.3 mmol of powdered NaOMe was added to the solution. After the deprotonation was completed, 0.3 mmol of Ni(II)$(ClO_4)_2$ dissolved in 5 mL of methanol was added dropwise. Deep-red crystals were obtained by diffusion of MeCN in the solvent system. Yield, 56%. ESI-MS *m*/*z*: 1493.72 $(M + H)^+$. Calcd for $C_{69}H_{57}N_6Cl_3O_{15}Ni_3 + H^+$: 1493.66. Anal. Calcd for $C_{69}H_{57}N_6Cl_3O_{15}Ni_3$: C 55.5, H 3.8, N 5.6. Found: C 55.3, H 3.6, N 5.6.

X-ray Crystallography. Crystallographic measurements were made using a Siemens P4 diffractometer with graphite-monochromated Mo Kα radiation (λ = 0.71073 Å) and a 12 kW rotating generator. The data were collected at 25 ± 1 °C. These structures were then defined and revised using the SHELXS-97 and SHELXL-97 (Sheldrick, 1997) software programs. The X-Seed (Barbour, 1999) program was used both as an interface to the SHELX programs, and to plot the figures. Crystallographic data including data collection, structure, composition, physical characteristics, and refinement are summarized in Table 1. Unfortunately, after numerous attempts to obtain single crystals suitable for analysis of complexes **4**, **9**, and **11**, we remained unsuccessful in this effort using current techniques and available equipment. Consequently, they are omitted from Table 1.

Table 1 data have been indexed and are included in the Cambridge Crystallographic Center (CCDC) database with the following reference numbers: CCDC-219495 (**1**), CCDC-219496 (**2**), CCDC-224539 (**3**), CCDC-212130 (**5**), CCDC-212129 (**6**), CCDC-219494 (**7**), CCDC-226897 (**8**), and CCDC-224540 (**10**). The indexed database contains additional supplementary crystallographic data for this paper and may be accessed without charge at http://www.ccdc.cam.ac.uk/conts/retrieving.html. The CCDC may contacted by mail at 12, Union Road, Cambridge CB21EZ, U.K., by fax at (44)1223-336-033, or by e-mail at deposit@ccdc.cam.ac.uk.

Results and Discussion

Initially, the chiral Robson-type macrocycles, *R,R*-H_2**L1,** and *R,R*-H_2**L2** (see Scheme 2), were prepared by the direct cyclocondensation between the chiral diamine and the corresponding aldehyde at 45 °C in MeOH or MeCN. However, the [2 + 2] product is difficult to purify due to the instability of the Schiff bases and contamination from other byproducts of the reaction.

In the presence of certain transition metal ions, the [2 + 2] macrocyclic complexes of *R,R*-H_2**L1** and *R,R*-H_2**L2** were found to form easily with high yields (>90%). This is because the metal ions readily utilize the bridging capacity of the phenol groups. For the investigation of the template effect of transition metal ions, Ni^{2+} was first employed due to its four planar coordination nature. The mono- and dinuclear Ni(II) complexes of *R,R*-H_2**L1** were successfully prepared by template condensation of *R,R*-DPEN with 2-hydroxy-5-methyl-1,3-benzenedicarboxaldehyde. Reaction of the dialdehyde and *R,R*-DPEN with 0.5 equiv of Ni(II) produced a yellow mononuclear complex (see complex **1** in Figure 1), whereas the reaction with 1 equiv of Ni(II) with the addition of Et_3N, creating a more basic condition, yielded a brown dinickel product (see complex **2** in Figure 1). The structures of these complexes were investigated by X-ray crystallography as shown in Figure 1.

The X-ray structure of the mononuclear Ni(II) cation of [(*R,R*-H_2L1)Ni(II)]$(ClO_4)_2$ (Complex 1 in Figure 1). The nickel ion occupies one N_2O_2 cavity, binding with two imine groups and two phenolic oxygen atoms. The geometry of the metal ion is planar, and the whole macrocycle adopts a saddlelike conformation. Elemental analyses in addition to ESI-MS procedures indicated that the macrocycle is not deprotonated. Upon deprotonation of the two phenol groups, the macrocyclic ligand can bind a second metal ion forming a homo- or hetero-dinuclear complex. The dinuclear Ni(II) complex [(*R,R*-**L1**)Ni_2(II)]$(ClO_4)_2$·2MeCN (complex **2** in Figure 1) changed from yellow to brown, presumably because of the charge transfer between the fully deprotonated phenolate groups and the Ni(II) ions. The cations occupy two chiral cavities (Figure 1), with each ion bound to four macrocyclic donors in the basal plane. The Ni(II)−Ni(II) distance (Ni1−Ni2, 2.865 Å) is short but is not representative of a typical Ni−Ni bond. The conformation of the macrocycle is very similar to that of structure **1**, and the dicationic

Table 1. Crystal Data and Structure Refinement for Complexes **1**−**3**, **5**−**8**, and **10**

	1	**2**	**3**	**5**	**6**	**7**	**8**	**10**
empirical formula	$C_{50}H_{44}Cl_2Ni$-N_6O_{10}	$C_{50}H_{45}Cl_2$-$Ni_2N_6O_{10}$	$C_{48}H_{44}Cl_2$-ZnN_4O_{12}	$C_{50}H_{44}Cl_2$-$Cu_2N_6O_{10}$	$C_{68}H_{91}Cl_4$-$Co_4N_8O_{30}$	$C_{35}H_{44}N_6$-PbS_2O_5	$C_{73}H_{68}N_8O_4$	$C_{34}H_{24}N_2O_2$
fw	1018.52	1437.65	1005.14	1086.89	1878.01	889.56	1117.98	492.55
cryst size (mm^3)	0.30 × 0.20 × 0.20	0.84 × 0.26 × 0.22	0.40 × 0.30 × 0.10	0.10 × 0.10 × 0.05	0.20 × 0.20 × 0.10	0.20 × 0.20 × 0.20	0.30 × 0.10 × 0.10	0.40 × 0.31 × 0.25
temp (K)	110(2)	110(2)	110(2)	110(2)	110(2)	110(2)	110(2)	110(2)
wavelength	0.71073 Å	0.71073 Å	0.71073 Å	0.71073 Å	0.71073 Å	0.71073 Å	0.71073 Å	0.71073 Å
cryst syst	monoclinic	tetragonal	monoclinic	orthorhombic	orthorhombic	triclinic	monoclinic	orthorhombic
space group	$P2_1$	$P4_3$	$P2_1$	$P2_12_12_1$	$P2_12_12_1$	$P1$	$P2_1$	$P2_12_12_1$
a (Å)	9.522(12)	10.2115(4)	13.3272(10)	9.6972(8)	16.970(5)	11.593(3)	13.7823(9)	12.011(4)
b (Å)	16.60(2)	10.2115(4)	11.3083(8)	10.4822(8)	19.821(5)	12.366(3)	29.0273(19)	18.521(7)
c (Å)	14.844(18)	43.848(3)	15.0979(11)	45.648(3)	23.093(5)	14.880(4)	16.1071(11)	22.708(8)
α (deg)	90	90	90	90	90	67.814	90	90
β (deg)	100.16(2)	90	98.0270	90	90	67.952	100.820(10)	90
γ (deg)	90	90	90	90	90	88.071	90	90
V ($Å^3$)	2310(5)	4572.3(4)	2253.1(3)	4640.1(6)	7768(3)	1816.3(8)	6329.3(5)	5052(3)
Z	2	4	2	4	4	2	4	8
D_{calc} (Mg/m^3)	1.464	1.566	1.482	1.556	1.606	1.627	1.173	1.295
abs coeff (mm^{-1})	0.604	1.010	0.734	2.760	1.067	4.808	0.073	0.081
F(000)	1056	2228	1040	2232	3884	889	2369	2064
θ range (deg)	1.39−28.53	0.93−27.52	1.91−28.32	3.87−59.06	2.04−25.00	1.61−25.00	1.90−25.00	2.47−25.00
reflns collected	22988	38628	19776	23938	41588	15029	52805	26382
indep reflns	10704 [R(int) = 0.0657]	10482 [R(int) = 0.0720]	9531 [R(int) = 0.0275]	6537 [R(int) = 0.0577]	13474 [R(int) = 0.3445]	11357 [R(int) = 0.0469]	22046 [R(int) = 0.0378]	8837 [R(int) = 0.0526]
abs correction	*a*	none	*a*	*a*	*a*	none	*a*	none
max and min transm	0.8888 and 0.8397	0.8077 and 0.4860	0.9303 and 0.7579	0.8743 and 0.7698	0.9008 and 0.8149	0.4464 and 0.4464	0.9927 and 0.9784	0.9801and 0.9684
refinement method on F^2	*b*	*b*	*b*	*b*	*b*	*b*	*b*	*b*
data/restraints/ params	10704/1/636	10482/1/636	9531/1/625	6537/0/631	13474/0/1004	11357/561/ 869	22046/46/1525	8837/516/689
GOF on F^2	1.060	1.051	1.045	1.026	1.003	1.123	1.003	0.945
final R indices[c] [$I > \sigma(I)$]	R1 = 0.0662, wR2 = 0.1482	R1 = 0.0458, wR2 = 0.0993	R1 = 0.0560, wR2 = 0.1406	R1 = 0.0354, wR2 = 0.0841	R1 = 0.0837, wR2 = 0.1543	R1 = 0.0307, wR2 = 0.0751	R1 = 0.0656, wR2 = 0.1605	R1 = 0.0491, wR2 = 0.1093
R indices (all data)	R1 = 0.0888, wR2 = 0.1566	R1 = 0.0514, wR2 = 0.1174	R1 = 0.0650, wR2 = 0.1486	R1 = 0.0398, wR2 = 0.0857	R1 = 0.3088, wR2 = 0.2219	R1 = 0.0349, wR2 = 0.0769	R1 = 0.1052, wR2 = 0.1974	R1 = 0.0690, wR2 = 0.1200
largest diff peak and hole	1.031 and −0.760 e $Å^{-3}$	0.558 and −0.739 e $Å^{-3}$	1.369 and −0.524 e $Å^{-3}$	0.463 and −0.307 e $Å^{-3}$	0.647 and −0.835 e $Å^{-3}$	1.543 and −1.264 e $Å^{-3}$	1.112 and −0.312 e $Å^{-3}$	0.226 and −0.280 e $Å^{-3}$

[a] Semiempirical from equivalents. [b] Full-matrix least squares. [c] $R1 = \sum||F_o| - |F_c||/\sum F_o$. $wR2 = \{[\sum(F_o^2 - F_c^2)^2/[\sum w(F_o^2)^2]]\}^{1/2}$.

Scheme 2

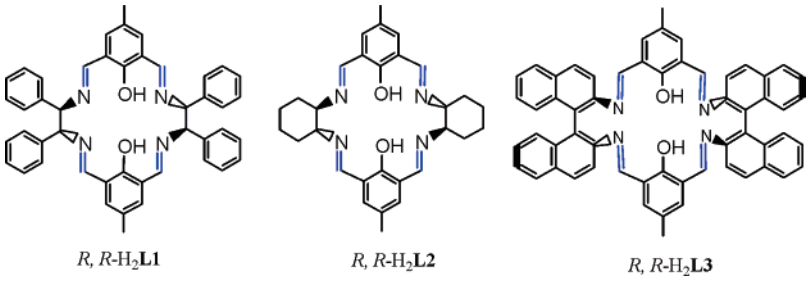

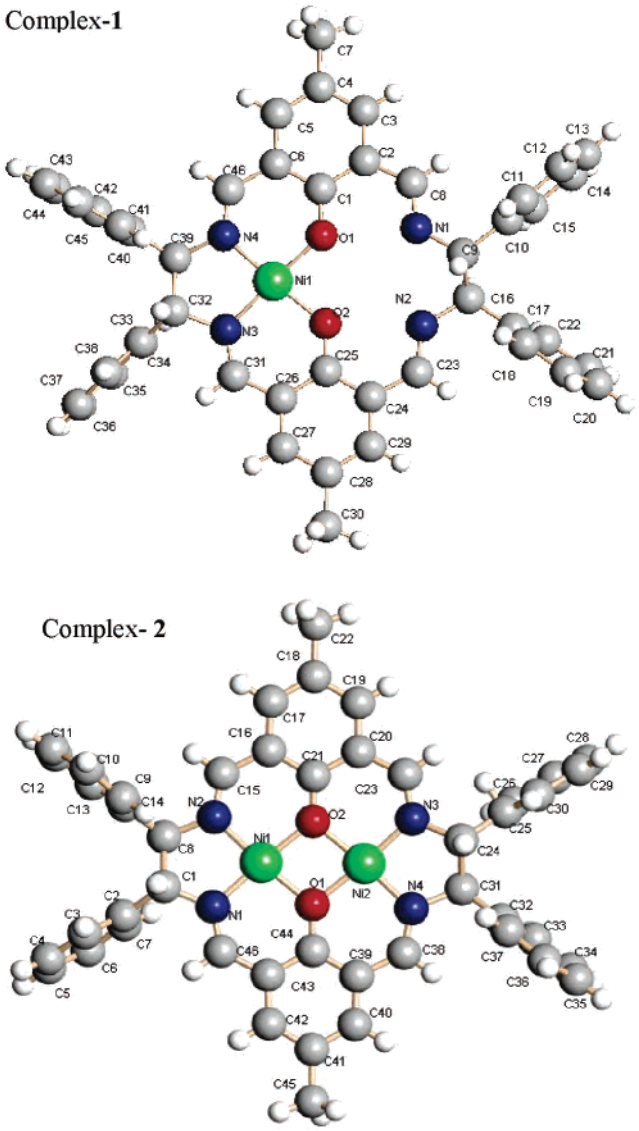

Figure 1. X-ray structure of mononuclear (complex **1**) and dinuclear (complex **2**) Ni(II) cationic complexes.

complex possesses an overall D_2 symmetry. However, the extension of the template condensation approach in the synthesis of *R*,*R*-H_2**L3** from *R*-BNDA and the dialdehyde proved unsuccessful. The ESI-MS spectrum of the resulting solution (see Scheme 3) indicated that no [2 + 2] complex could be identified. We speculate that there are two possible explanations for this phenomenon: (1) a near planar four-coordination geometry of N_2O_2 cannot be formed when binding with Ni^{2+}; (2) the structural rigidity and/or axial chirality of BNDA may not allow for the formation of *R*,*R*-H_2**L3**.

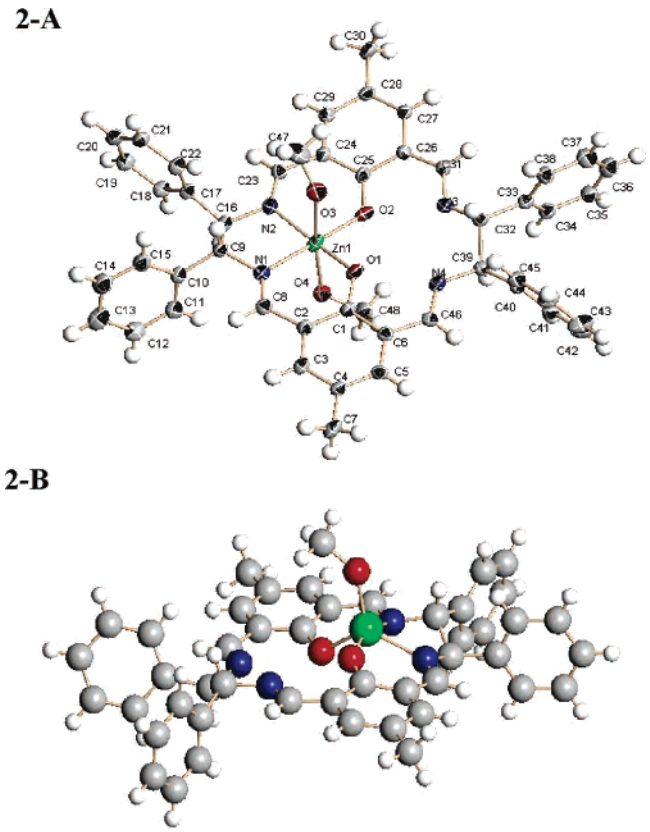

Figure 2. X-ray structure of **3**: (A) major species; (B) minor species.

Other than nickel(II), zinc(II) can also serve as an effective template for the formation of *R*,*R*-H_2**L1**, but the structural feature of this cationic molecule is quite unusual. In the presence of 0.5 equiv of Zn(II), a mononuclear complex [(*R*,*R*-H_2**L1**)Zn(II)]$(ClO_4)_2$·2MeOH (**3**) was obtained (see Figure 2). The crystal structure contains two different species, namely **A** and **B**, which interact with one or two methanol molecules along the axial direction, respectively. The coordination environment around Zn(II) in **A** is octahedral and in **B** square pyramidal. These observations can be attributed to the enlarged ionic radius of Zn(II) (0.74 Å) as compared to Ni(II) (0.69 Å). Upon deprotonation of the two phenol groups followed by charging with the second zinc ion, a dizinc complex [(*R*,*R*-**L1**)Zn_2(II)]$(ClO_4)_2$ (**4**) was obtained.

The coordination of Cu(II) to this chiral macrocycle is much stronger than that of Ni(II) and Zn(II). Irrespective of whether base was introduced, the product is always the dicopper(II) complex. [(*R*,*R*-**L1**)Cu_2(II)]$(ClO_4)_2$·2MeCN (**5**) that was crystallized from MeCN was characterized by X-ray

Scheme 3

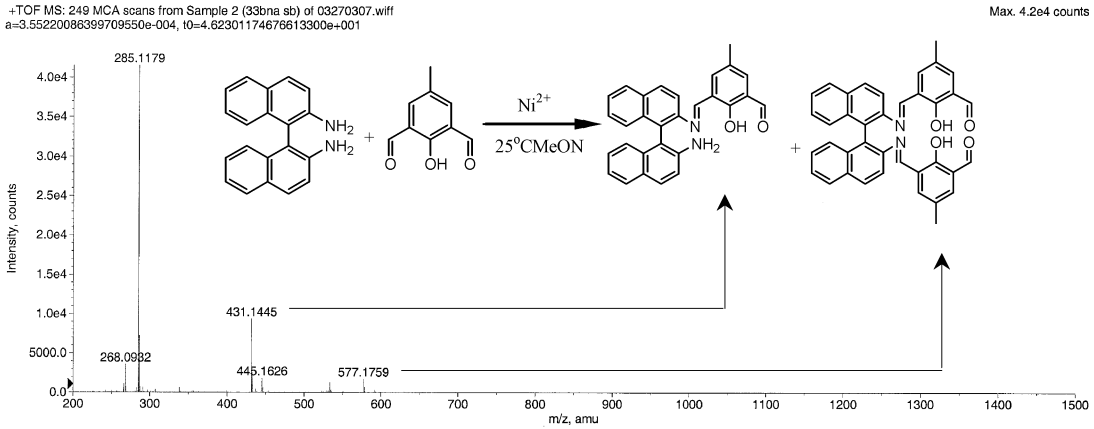

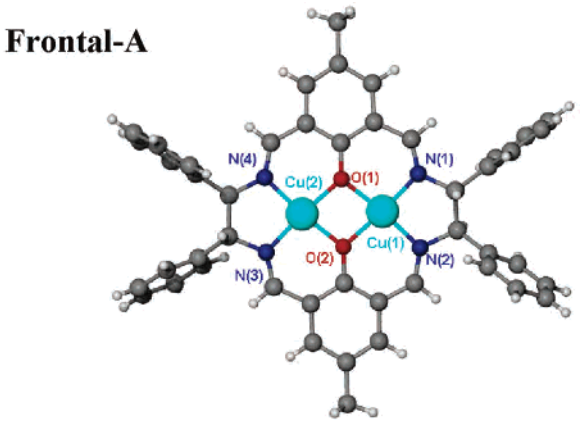

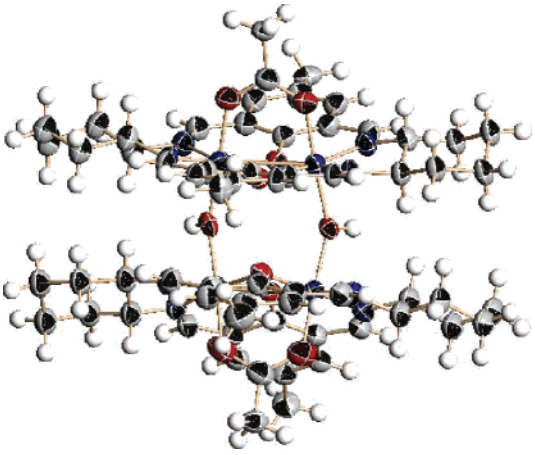

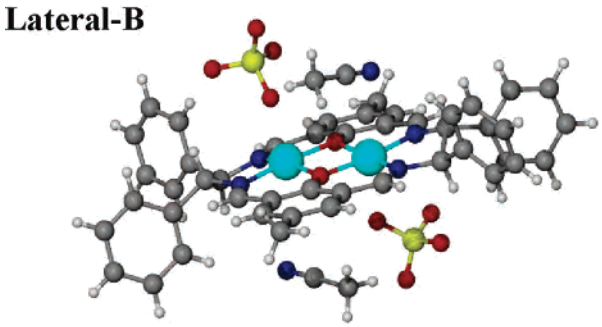

Figure 4. ORTEP drawing of complex **6**. Lateral view of the cationic core.

Figure 3. X-ray molecular structure of **5**: (A) frontal perspective view; (B) lateral perspective view.

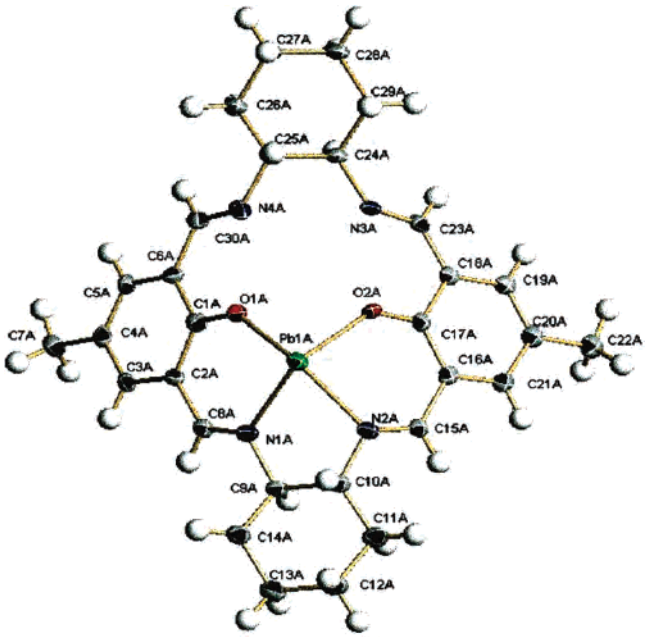

Figure 5. Perspective view of the X-ray structure of **7**.

analysis (see Figure 3). The crystal structure reveals a dinuclear structure bearing two Cu(II) centers bridged by two phenolic oxygen. Each Cu(II) cation is entrapped in the nine-membered coordination compartment of the 18-membered macrocycle, and the Cu(II) centers are four-coordinate. On each side of the molecular platform, a coordinated MeCN molecule and a ClO_4^- anion were observed. The overall geometry of the molecule is a basal plane with four chiral C−H bonds nearly perpendicular to the N_4O_2-plane.

Similar template effects of Ni(II), Cu(II), and Zn(II) were observed in the construction of the mono- and dinuclear complexes of *R*,*R*-H_2**L2**. This approach was studied to include the syntheses of the air-sensitive dinuclear complexes of Mn^{2+}, Fe^{2+}, and Co^{2+}. These metal ions were found to be effective in forming the corresponding dinuclear complexes which in turn react with O_2 to afford the dioxygen adducts. Although no single crystal structures were obtained, the elemental analyses and ESI-MS spectra confirm the formation of the dinuclear complexes. Significantly, oxida-

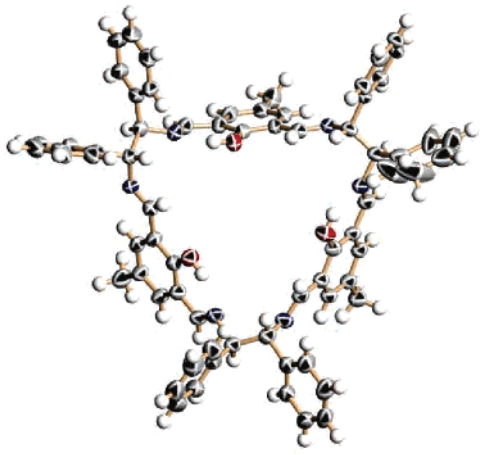

Figure 6. X-ray structure of *R*,*R*-H_3**L4**.

tion of the dicobalt(II) complex [(*R*,*R*-**L2**)Co_2(II)]$^{2+}$ occurred in air when a Lewis acid (i.e., acetic acid) was added dropwise. This led to the isolation of the chiral tetranuclear Co(III) complex [(*R*,*R*-**L2**Co_2(III))$_2$$(OH)_2$$(OAc)_2$]$(ClO_4)_4$·4$CH_3$OH (**6**), which was characterized crystallographically as shown in Figure 4. The complex could best to be described as a "dimer of dimer" structure constructed via the efficient spontaneous self-assembly of two tetra-Schiff-base scaffolds and two hydroxyl groups. This structure represents one of the rare examples of artificial chiral tetranuclear supermolecules.[12]

Consequently, we investigated the template effects of larger metal ions such as Cd(II), Pb(II), and La(III) (ionic radius 0.95, 0.119, and 0.116 Å, respectively). The outcome of these investigations clearly demonstrates that only mononuclear macrocyclic complexes can be successfully prepared with these metal ions. This behavior is significantly different from what was observed in the template synthesis of traditional Robson-type Schiff base macrocyclic complexes, which are highly template dependent. For example, Mg^{2+} may result in a tetranuclear complex, whereas Cu^{2+} creates a dinuclear complex.[13] This phenomenon can be related directly to the structural features of the linear diamine which lacks structural rigidity and chirality. In the synthesis of lead(II) complexes of *R*,*R*-H_2**L2**, the addition of 1 equiv of Pb(II) salt results in the formation of a mononuclear complex with a high yield (over 85%). It is important to note that the presence of more Pb(II) ions does not improve the yield given that the resulting complex persists as a mononuclear complex regardless of the availability of more Pb(II) ions. The cause of this phenomenon is readily explained by the limited cavity size of the macrocycle and the physical impossibility of accommodating additional large Pb^{2+} ions. The crystal structure of [Pb(II)**L1**]$(SCN)_2$ (**7**) reveals entrapment of a Pb(II) cation in the nine-membered coordination compartment of the 18-membered macrocycle H_2**L2** (see Figure 5). Pb(II) is tetracoordinate, bound to two phenolate oxygens and two diamine nitrogens. The coordination environment can be described as a distorted square plane. Within the macrocycle, Schiff base bonds are essentially coplanar with the adjacent phenolic aromatic rings, and the Pb(II) ion is slightly out of the plane due to its large ion size.

The template effects of alkaline metal ions were also

Scheme 4

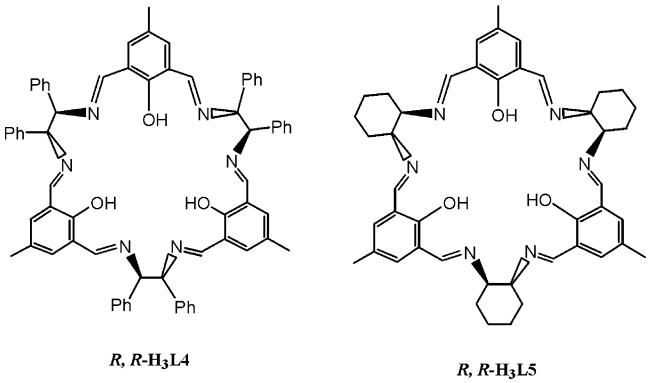

R, *R*-H_3L4 *R*, *R*-H_3L5

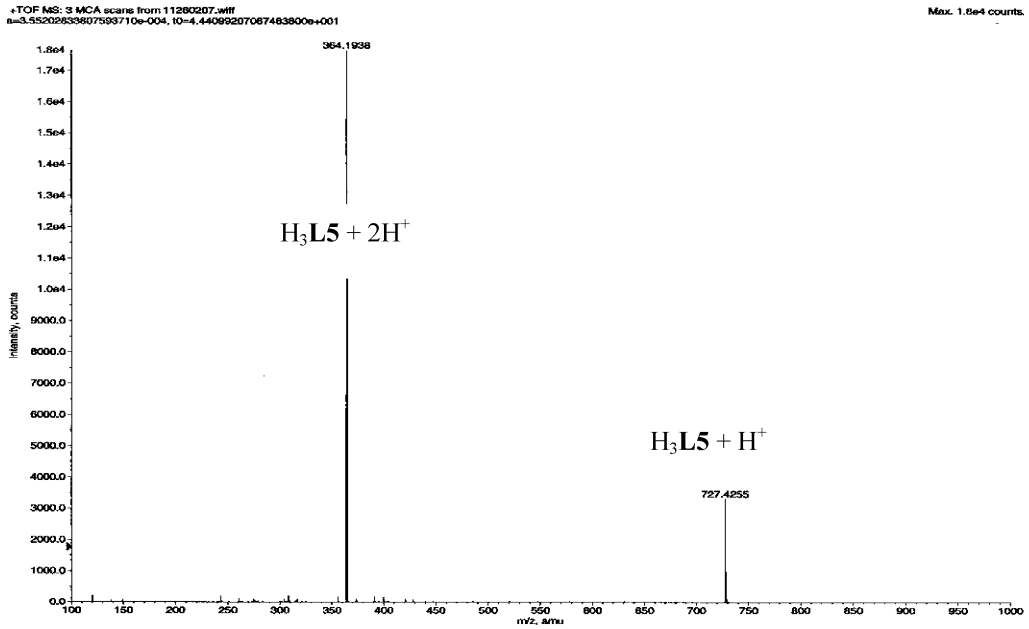

Figure 7. ESI-MS spectrum of **9**.

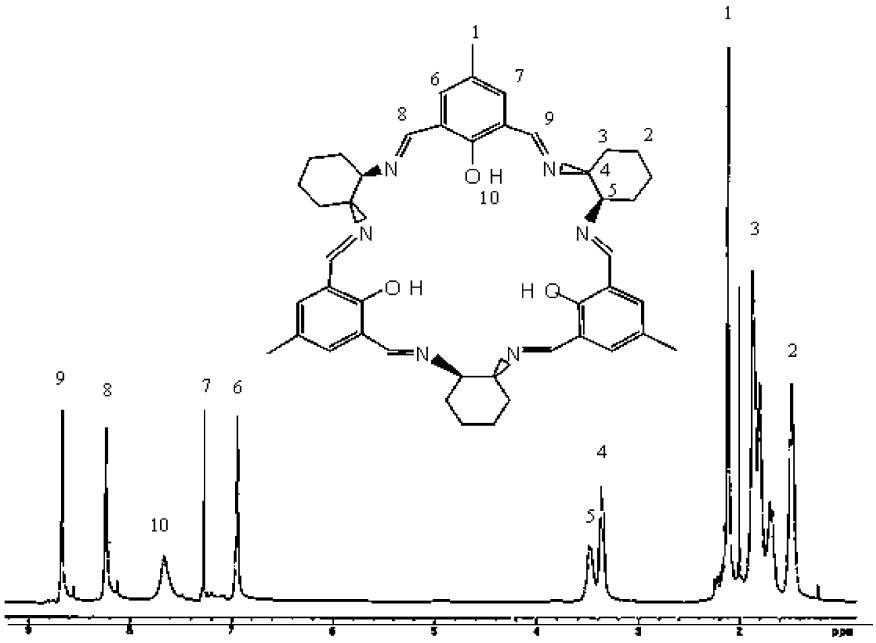

Figure 8. 500 MHz ^{1}H NMR spectrum of **9**.

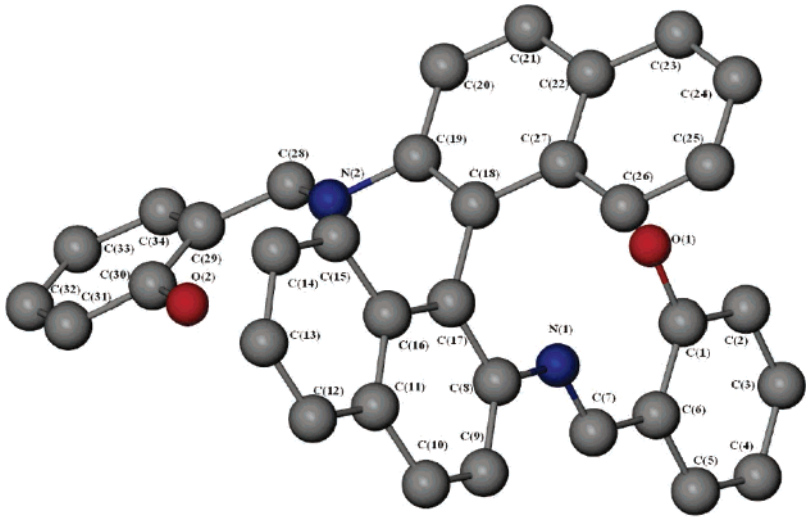

Figure 9. Crystal structure of compound **10**.

investigated. In contrast, Na^+, K^+, Rb^+, and Cs^+ showed no template effects in the formation of the macrocycles. The metal free [3 + 3] type chiral Schiff base macrocycle, *R*,*R*-H_3**L4** (**8**) and *R*,*R*-H_3**L5** (**9**), can be prepared in the presence of an excess of alkaline and even alkaline earth metal ions (see Scheme 4). In fact, **8** and **9** can be constructed via an efficient self-assembly method. The single crystal of **8** was prepared by slow evaporation of a solvent mixture (MeOH/CH_2Cl_2, 1:1) in the present of $NaClO_4$. The most striking structural feature of the chiral oligomeric macrocycle (Figure 6) is the vaselike tridimensional conformation, which is quite different from the conformation of normal achiral Schiff base polyaza macrocycles. As an analogue of the genuine calix-[*n*]arenes ($n = 3$), "calixsalen", the lower rim of the vase consists of methyl-substituted benzene fragments, and the upper rim contains the benzene rings from the diphenylethylenediamines. This represents an overall C_3 symmetry.

From the kinetic point of view, condensation reaction of dialdehydes with linear diamines generally affords polymeric Schiff base products including the [1 + 1], [2 + 2], [3 + 3], and [4 + 4] macrocycles and other polymeric Schiff base compunds,[14] depending upon the reactants and the template conditions. In this work, by using a rigid dialdehyde and a rigid chiral diamine, the self-assembly of 3 + 3 chiral macrocycle was highly efficient (>95%). ESI-MS spectrum of H_3**L5** (*m*/*z* [H_3**L5** + H^+], 727.42; [H_3**L5** + $2H^+$], 364.19). Figure 7 shows that the trimeric macrocycle was obtained

(12) (a) Olenyuk, O.; Whiteford, J. A.; Stang, P. J. *J. Am. Chem. Soc.* **1996**, *118*, 8221. (b) Stang, P. J. Olenyuk, B. *Acc. Chem. Res.* **1997**, *30*, 502. (c) Bu, X. H.; Morishita, H.; Tanaka, K.; Biradha, K.; Furusho, S.; Shionoya, M. *Chem. Commun.* **2000**, 971.

(13) Mohanta, S.; Nanda, K. K.; Werner, R.; Haase, W.; Mukherjee, A. K.; Dutta, S. K.; Nag, K. *Inorg. Chem.* **1997**, *36*, 4656.

(14) (a) Guerriero, P.; Vigato, P. A.; Fenton, D. E.; Hellier, P. C. *Acta Chem. Scand.* **1992**, *4*, 1025. (b) Chen, D.; Martell, A. E. *Tetrahedron* **1991**, *47*, 6895. (c) Aspinall H. C.; Black, J.; Dodd, I.; Harding, M. M.; Winkly, S. *J. Chem. Soc., Dalton Trans.* **1993**, 709. (d) Guerriero, P.; Tamburini, S.; Vigato, P. A. *Coord. Chem. Rev.* **1995**, *139*, 17.

Scheme 5

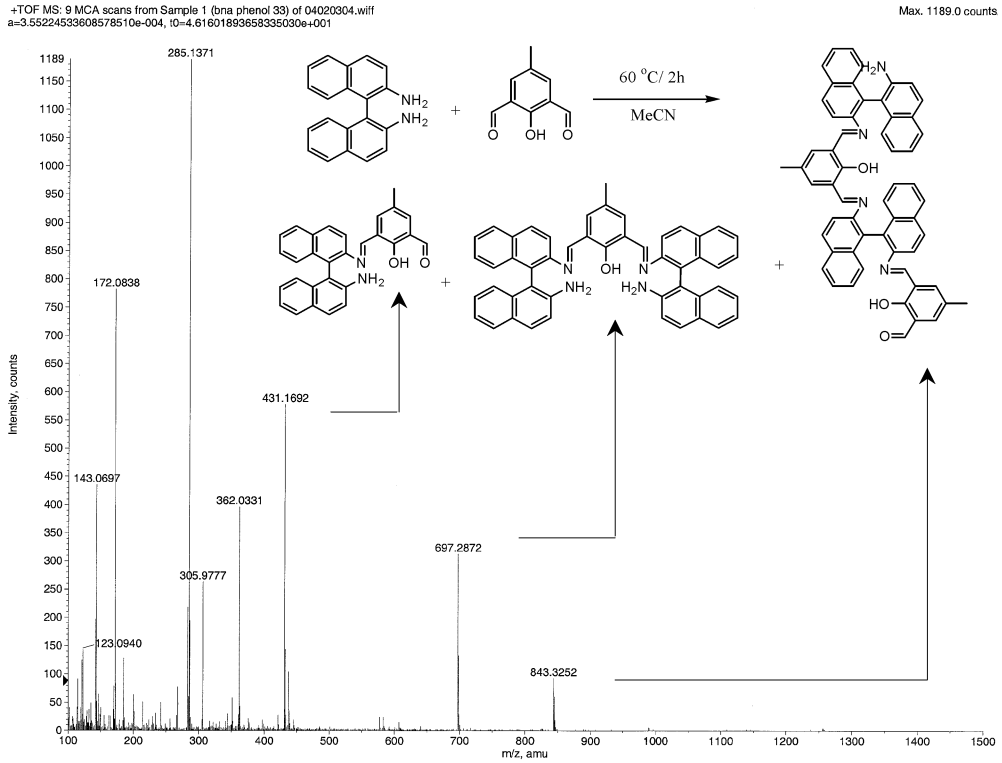

Scheme 6

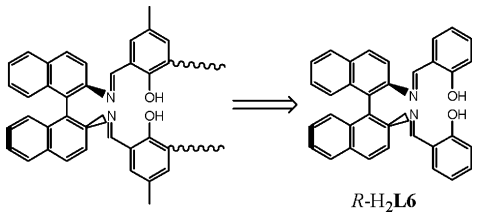

exclusively, without any contamination of [1 + 1], [2 + 2], or [4 + 4] byproducts. The 500 MHz ^{1}H NMR spectrum of the 27-membered macrocycle clearly indicates the existence of two kinds of chiral carbon by observing two N−C−H signals at 3.38 and 3.52 ppm, and the split imine signals at 8.21 and 8.64 ppm, respectively (Figure 8, with the numbering system in the inset). The integrations are in the ratio of approximately 1:1 and further substantiate the C_3 symmetric nature of the calixsalen molecule.

On the basis of this success, BNDA was utilized to synthesize the corresponding trimeric calixsalen. However, the direct condensation approach appears to be unsuccessful. The circular [2 + 2] molecule could not be assembled despite numerous attempts. When viewed in the ESI-MS spectrum (Scheme 5), the [2 + 2] structural components fail to connect using direct condensation. Similarly, the circular [3 + 3] form does not exist. Instead, the open chain compounds of [1 + 1], [1 + 2], and [2 + 2] condensation were observed. To gain further insight into the underlying mechanism in this reaction, we synthesized a model molecule of *R*-H_2**L6** (**10**) to mimic the local geometry around *R*-BNDA (Scheme 6). As was indicated by the X-ray structure of *R*-H_2**L6** (Figure 9), the affiliated phenol groups are constrained to remain on each side of the pivot due to the energy barrier that exists in the chiral diamine. The failure of the self-assembly process can be explained by the restricted rotation around the aryl−aryl bond.

Subsequently, the coordination properties of the calixsalens were investigated. Formally, the trinuclear transition metal complexes of **8** can be generated by the direct reaction of

Scheme 7

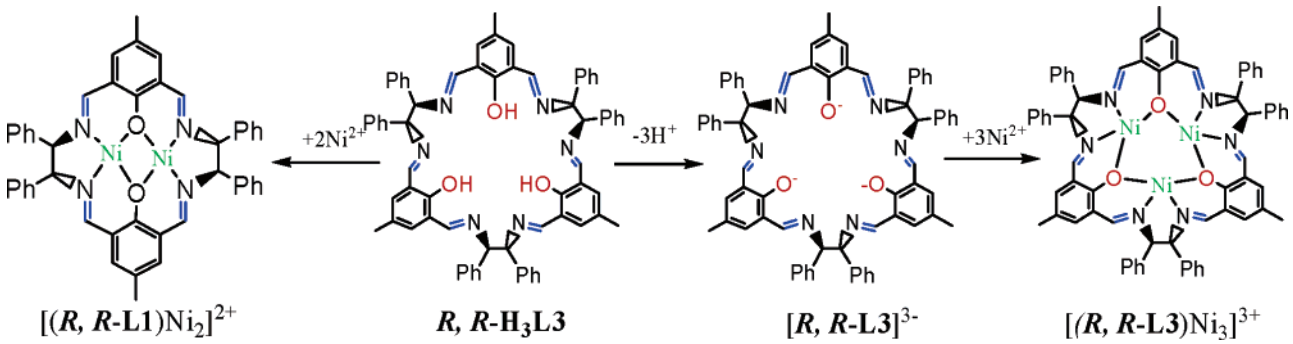

Scheme 8. Molecular Structures of Mono-, Di-, and Trinuclear Ni(II) Complexes Obtained by Semiempirical PM3 Method[a]

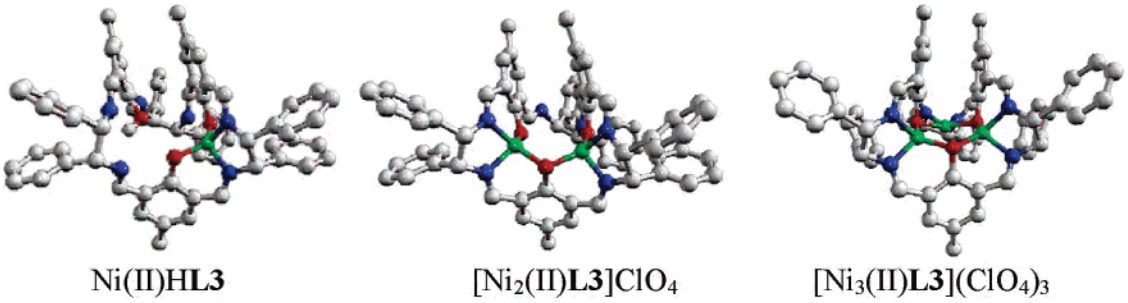

Ni(II)H**L3** $[Ni_2(II)\mathbf{L3}]ClO_4$ $[Ni_3(II)\mathbf{L3}](ClO_4)_3$

[a] Red, oxygen; blue, nitrogen; green, nickel; gray, carbon.

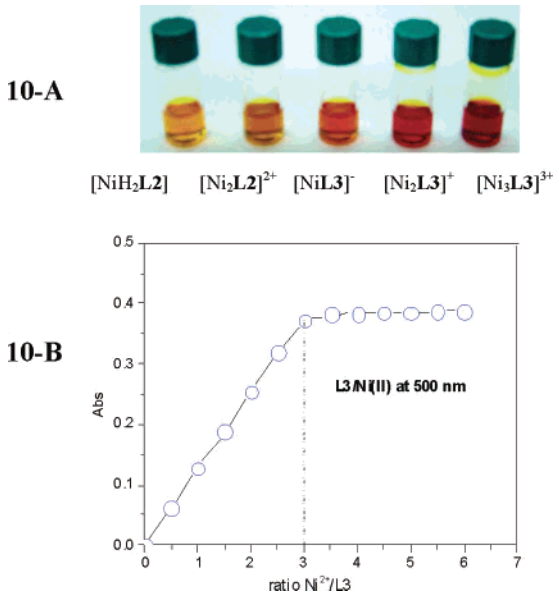

Figure 10. (A) Color change of the Ni(II) complexes of *R,R*-H_2**L1** and *R,R*-H_3**L3**. (**B**) Spectrophotometric titration of Ni-**L3** system: [**L3**] = 6.67 mM (MeOH/CH_2Cl_2, 1:1), absorption was monitored at 500 nm.

the free ligand with specific transition metal ions such as Cu(II), Ni(II), or Zn(II). However, this results in the cleavage of the trimeric macrocycle and the formation of the dinuclear species of *R,R*-H_2**L1** (Scheme 7). The ring contraction product is considered to be the thermodynamic product. Surprisingly, however, reaction of the Schiff base salt, Na_3**L3**, with Ni(II) can produce mono-, di-, and trinuclear complexes, $[(R,R\text{-}\mathbf{L3})Ni_3](ClO_4)_3$ (**11**), depending on the ligand/metal ion ratio. Molecular modeling study shows that the energy-minimized conformation of the complexes is highly distorted and the vaselike confirmation cannot be maintained (Scheme 8). Upon binding with the metal ions, one of the three phenol groups of the macrocyclic ligand reverses its direction. Successful preparation of these compounds was confirmed by ESI-MS and elemental analyses. The stepwise binding behavior of Na_3**L3** with Ni(II) was monitored by means of spectrophotometric titration (Figure 10). The variation of absorption maximum at 500 nm indicates that Na_3**L3** binds with Ni(II) in three steps before reaching saturation. This phenomenon explicitly illustrates the critical role protons play in the rearrangement of the macrocycle in coordination with metal ions.

In summary, we have reported the systematic results of the synthesis of a series of chiral calixsalen macrocycles and the Robson-type mono-, di-, tri-, and tetranuclear chiral macrocyclic complexes. Much of the unusual synthetic and X-ray structural information generated by this report should be of significant use in a variety of applications within the domain of bioinorganic chemistry. The utilization of these chiral macrocycles and chiral multinuclear complexes in enzyme-like asymmetric catalysis and in the interaction with biological molecules will be published soon.

Acknowledgment. This program was financially supported by The Welch Foundation, Grants A-0259 and A-084.

Supporting Information Available: Complementary X-ray structural data for **1**, **2**, **3**, **5**, **6**, **7**, **8**, and **10**. This material is available free of charge via the Internet at http://pubs.acs.org.

IC049181M